Proceedings of the 20th International Conference on Soil Mechanics and Geotechnical Engineering– Rahman and Jaksa (Eds)

Permanence of enhanced compressibility of bio-cemented sands with stress and time

Permanence de la compressibilité améliorée des sables bio-cimentés avec l'évolution des contraintes et du temps

Ray Harran & Dimitrios Terzis & Lyesse Laloui
Laboratory of Soil Mechanics, Swiss Federal Institute of Technology, Lausanne, Switzerland. ray.harran@epfl.ch

ABSTRACT: Microbially Induced Calcium Carbonate Precipitation (MICP) has been extensively studied as a promising ecological soil improvement alternative. While abundant characterizations of the peak and softening behaviors of bio-cemented soils exist, less is known about its uniaxial deformability, while it remains central for most envisaged applications. In this study, novel aspects related to the compressibility of bio-cemented sands are covered, namely its enhancement following MICP treatment of two sands, and its permanence with increasing stresses, and its evolution with time. Through an incremental loading and a sustained loading series of one-dimensional compression tests, a more complete characterization of the deformability was targeted, covering the influence of initial compactness, treatment level, and the first adaptation of the porosity-cement ratio from artificially cemented soils to bio-cement. In addition, the first characterization of the delayed deformation with time of MICP treated materials along with its interdependence with stress are examined.

RÉSUMÉ : L'amélioration des sols par le biais de précipitation microbienne contrôlée de carbonate de calcium (MICP) a été extensivement étudiée comme l'alternative écologique la plus prometteuse. S'il existe de nombreuses études qui couvrent le comportement des sols bio-cimentés au pic de force et à la phase d'adoucissement qui s'en suit, la déformabilité uniaxiale reste toutefois moins connue, malgré sa place centrale dans la plupart des applications envisagées. Dans cette étude, de nouveaux aspects liés à la déformabilité des sols bio-cimentés sont abordés, notamment l'amélioration de la compressibilité de deux sables suite à leur traitement, et sa permanence avec des contraintes croissantes et son évolution dans le temps. Grâce à deux séries de tests à chargement incrémental et de compression unidimensionnelle sous charge constante, une caractérisation plus globale de la déformabilité a été ciblée, couvrant l'influence de la compacité initiale, du niveau de traitement, ainsi que la première adaptation au bio-ciment du rapport de porosité-ciment originaire des sols artificiellement cimentés. Également, la première caractérisation de la déformation différée avec le temps ainsi que son interdépendance avec les contraintes sont examinées.

KEYWORDS: MICP, bio-cementation, soil improvement, compressibility, creep.

1 INTRODUCTION

Bio-stabilization of new or existing structures is one of the most promising applications of MICP as a soil improvement technique, and is essentially governed by settlement criteria instead of ultimate strength. Compared to the abundance of studies dedicated to large strains, peak strength and softening, a more global understanding of the deformability of bio-cemented soils as a novel geomaterial is needed. The present study aims to characterize the impact of stress and time on the permanence of the enhanced compressibility of two sands following an MICP treatment.

For artificially cemented soils in general, the density and cement content were shown to hold a key role in governing the mechanical behavior (Wei and Ku 2020). Conveniently, a porosity to cement ratio was proposed for Portland cemented soils (Consoli et al. 2012) to express this density-cementation dependence, and is applied for the first time in this work to bio-cemented cases, since relying solely on gravimetric calcite contents is not sufficient (Lee et al. 2013). In the few studies covering the compressibility of bio-cemented soils, even very low cementation was seen to be impactful (Feng and Montoya 2014), and the deformability could indirectly be followed using S-wave velocities (Lin et al. 2016). MICP was also reported to mitigate compressibility problems of coal-ash (Montoya et al. 2019). Few studies however focused on the comparison between different sands, initial densities and cement contents on the enhancement of the deformability and its subsequent evolution with incremental loading in k_0 conditions.

Creep of soils is one of multiple scopes relative to time-dependent phenomena, defined as deformations under sustained load in the course of time. Existing studies focusing on time-dependent characteristics of artificially or bio-cemented soils, usually cover scopes that do not fit a sustained load framework, but rather target other considerations such as, the curing time on strength buildup or dissolution problems (Croizé et al. 2010). To the author's best knowledge, no observations of the creep-like behavior of bio-cemented soils exist, and the permanence of the enhanced state due to the treatment under a sustained load remains unknown.

The present study aims to characterize the deformability of bio-cemented sands, by addressing the enhancement conveyed due to an MICP treatment and how it is retained with increasing stresses and time evolution.

2 MATERIALS AND METHODS

2.1 *Samples Preparation and Treatment*

Two types of SP (ASTM D2487) silica sands were adopted namely, a fine (Itterbeck, Netherlands, D_{50} = 185 μm) and a medium (Bernasconi, Switzerland, D_{50} = 363 μm) grained sands, dry pluviated and manually tamped in plastic recipients (d = 60 mm, h = 120 mm).

MICP treatment was based on batch injections of two solutions: a bacterial and a cementation solution. The biological preparation is similar to that presented in (Terzis and Laloui 2019). Lyophilized *Sporosarcina Pasteurii* (ATCC 11859) was the adopted urea-hydrolyzing microorganism, rehydrated under aerobic conditions at 25°C in a broth consisting of urea (0.3 M) and peptone (5 g/L), monitored with Electric Conductivity (EC) measurements. The cementation solution had an equimolar concentration (0.5 M) of urea and calcium chloride. Batches of

140 mL (1.2 pore volume) were injected using a peristaltic pump (5 mL/min) by alternating the input-output inlets in order to maximize the specimens' homogeneity. Following a first inoculation and 12 h retention time for bacterial attachment, cementation solutions were injected with systematic pH and EC measurements carried out on both influent and effluent samples. Bacterial solution batches were reintroduced to the system when needed, in order to compensate for observed drops in efficiency due to decay or washout of bacteria. At the conclusion of the treatment, samples were flushed with distilled water and oven dried before testing. At the conclusion of the mechanical tests, the calcium carbonate content was determined using a gravimetric approach, as the difference of dry mass measured before and after acid washing (HCl at 1 M).

2.2 *Testing Plan*

Two complementary testing series allowed to cover the stress and time considerations in saturated uniaxial laterally constrained loading conditions.

In the Incremental Loading Series (ILS), 8 samples of medium sand and 9 samples of the fine sand were tested in one-dimensional compression (d = 60 mm, h = 15 mm) with varying initial densities and cementation levels. Each test consisted of 8 incremental loading steps 15, 60, 125, 250, 500, 60, 500 and 1000 kPa, each lasting around 24h with a stabilization verification (10 μm/12h threshold) using LVDTs with an accuracy of one micron.

Table 1. Experimental series plan and sample characteristics

Test No.	Sand	$CaCO_3$ content (%)	Void ratio e_i before MICP	Void ratio e_0 after MICP	η / C_{iv}
Incremental Loading Series (ILS)					
ILS-M-0-1	Medium	0	0.70	0.70	N/A
ILS-M-0-2	Medium	0	0.74	0.74	N/A
ILS-M-3-1	Medium	3	0.74	0.70	24.5
ILS-M-3-2	Medium	3	0.75	0.70	24.0
ILS-M-3-3	Medium	3	0.76	0.71	24.4
ILS-M-3-4	Medium	3	0.78	0.73	25.0
ILS-M-4	Medium	4	0.79	0.73	21.9
ILS-M-5	Medium	5	0.83	0.74	16.6
ILS-F-0-1	Fine	0	0.56	0.56	N/A
ILS-F-0-2	Fine	0	0.59	0.59	N/A
ILS-F-4	Fine	4	0.63	0.56	14.0
ILS-F-5	Fine	5	0.61	0.53	11.7
ILS-F-6-1	Fine	6	0.54	0.46	9.8
ILS-F-6-2	Fine	6	0.62	0.54	11.0
ILS-F-7-1	Fine	7	0.58	0.48	8.4
ILS-F-7-2	Fine	7	0.55	0.45	7.5
ILS-F-8	Fine	8	0.64	0.52	7.8
Sustained Loading Series (SLS)					
SLS-2-40	Medium	2	0.76	0.72	32.4
SLS-3-40	Medium	3	0.78	0.73	26.6
SLS-4-40-1	Medium	4	0.84	0.79	24.7
SLS-4-40-2	Medium	4	0.84	0.78	21.5
SLS-0-400	Medium	0	0.77	0.77	N/A
SLS-2-400-1	Medium	2	0.74	0.71	42.0
SLS-2-400-2	Medium	2	0.80	0.77	40.8
SLS-3-400-1	Medium	3	0.79	0.74	27.0
SLS-3-400-2	Medium	3	0.79	0.74	23.9
SLS-4-400	Medium	4	0.76	0.70	21.1

In complement, a Sustained Loading Series (SLS) consisted of maintaining a single uniaxial low (40 kPa) or high (400 kPa) stress over 10 samples (d = 50 mm, h = 20 mm) of the medium sand in laterally constrained conditions for a duration which varied between 75 or 90 days. Displacement readings were conforming with ASTM D2435 in the first 24h and then had a frequency of 1 reading per day.

Table 1 summarizes the characteristics of the samples and the testing plan, with a nomenclature showing the testing series (ILS or SLS), sand type (M or F), followed by the determined cementation level (range 0-8%). For the SLS, the sustained stress level (40 or 400 kPa) is also indicated.

3 RESULTS

3.1 *Stress Dependence*

As shown in Fig. 1-2, it can be seen when comparing the bio-cemented specimens to the natural untreated states at similar void ratios, that the MICP treatment reduced the accumulated axial strains at different stress levels. For example, for the medium sand, ε_a at 1000 kPa is reduced from 2.5% for the untreated to 1 and 1.5% respectively for treated samples with $CaCO_3$ contents of 4 and 5% (ILS-M-0-2, ILS-M-4 and ILS-M-5 at the same void ratio after treatment e_0 = 0.74). Similarly, for the fine sand, ε_a was reduced from 2.1% to 1.6% at a bond content of 4% (ILS-F-0-1 and ILS-F-4 at the same void ratio after treatment e_0 = 0.56). This enhancement is attributed to both the densification effect and bonding conveyed by the MICP treatment.

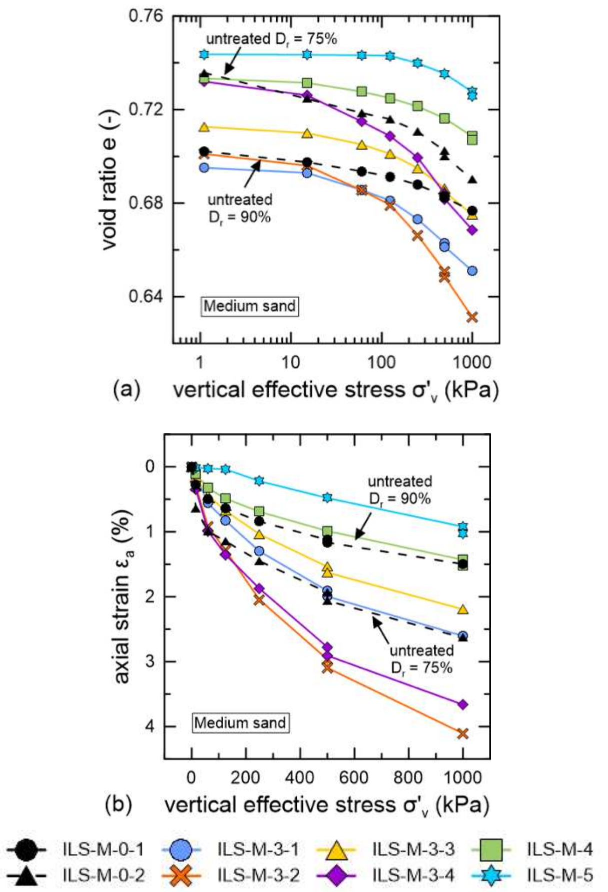

Figure 1. Variation of (a) void ratio and (b) axial strain with vertical effective stress for medium-grained sand

Initially at low stresses, the degree of reduction in ε_a seems to depend solely on the specimen's $CaCO_3$ content with no effect of the original void ratio, inferring that the bonding is the primary contributor at this stage. As stresses increase, results progressively diverge and eventually, at the highest applied stress of 1000 kPa, the recorded ε_a is influenced by both treatment level and initial density. For instance, ILS-M-0-2 and ILS-M-3-1 (both at the same void ratio before treatment $e_i = 0.74$), and ILS-F-0-1 and ILS-F-7-2 (both at the same void ratio before treatment $e_i = 0.56$) converge gradually towards the same ε_a. With a progressive damage caused with increasing stress, the bond contribution to the overall response was gradually taken over by compacity, typical to granular materials. The response was thus dependent on initial compactness, treatment level, and accumulated damage, itself a function of the treatment efficiency (number of induced active bonds) and applied stress. For almost all cases, a continuous accumulation of deformation was observed, without immediate collapse, and overall, the behavior of bio-cemented and Portland cemented sands are comparable at similar compactness and bond content (Yun and Santamarina 2005).

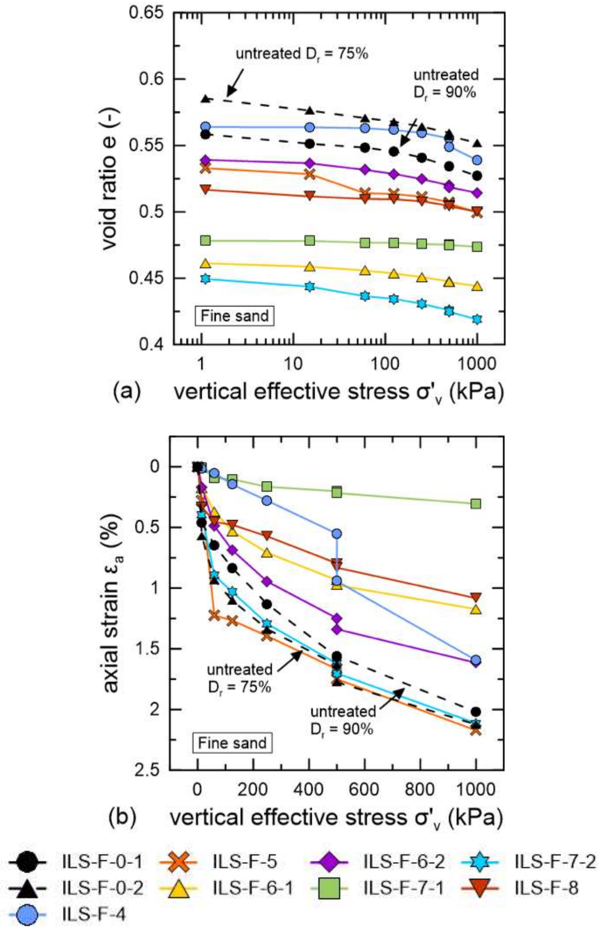

Figure 2. Variation of (a) void ratio and (b) axial strain with vertical effective stress for fine-grained sand

An application of the η / C_{iv} ratio to the tested samples is shown in Fig. 3, with a power law used to fit the measured strains as proposed in other studies (Consoli et al. 2012). For the medium sand, initially at low stresses, satisfactory relationships are obtained ($R^2 > 0.9$), but whose deterioration is observed in the form of a degradation front as stresses increase, with the damage of bonds and formation of compaction bands. After significant damage has taken place, any correlations of mechanical parameters with bond content (either in gravimetric terms or volumetric) is not suitable, due to the permanent loss of active bonds, no longer contributing to the response. Poor correlations are noted for the fine sand, notably due to the narrow margin of η / C_{iv} values and since the MICP treatment was possibly less efficient, where a high percentage of $CaCO_3$ was recorded but with fewer active bonds, as sometimes reported in other works (Terzis and Laloui 2018).

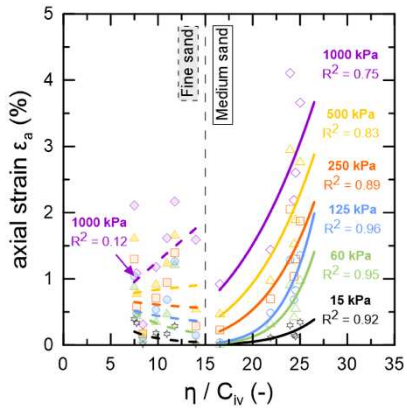

Figure 3. Variation of accumulated axial strain with porosity to cement ratio at different stress levels for medium and fine-grained sands

3.2 *Time Dependence*

A typical result of a single loading step is presented in Fig. 4, showing a representative response of both treated and natural states compared at a low (60 kPa) and high (1000 kPa) stresses. For both sands, in their untreated state, the major contribution to total recorded deformation is immediate settlement, as more than 90% of total ε_a is reached immediately after the load is applied. Similar observations are noted at 60 kPa for the treated state, showing that MICP did not significantly alter the behavior at this stage. At 1000 kPa however, clearly, the proportion of delayed compression is higher for bio-cemented samples, as immediate settlement only contributed to about half the total ε_a of that step. This observation can be evaluated using the coefficient of secondary compression (C_α), as the slope of the line post-primary consolidation.

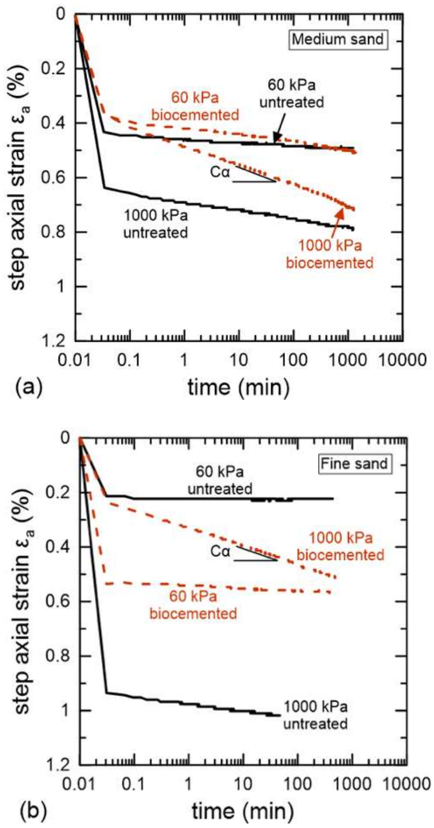

Figure 4. Loading steps at 60 and 1000 kPa of treated and untreated states for (a) medium and (b) fine-grained sands

Values of C_α at different steps are reported in Fig. 5. When looking at the natural sands, the values are higher for a looser state and increase with increasing stresses. MICP treated samples followed similar trends but with a different magnitude. First at the lower stress range, C_α values of treated samples are identical or even lower than the comparable loose state they started from before the treatment. At higher stresses however, the values exceed those of the untreated states and in some cases (ILS-M-3-2 and ILS-F-4), could attain a 3-fold increase at 1000 kPa.

C_α values of the SLS were comparable to those obtained from the ILS. However, in order to better isolate the evolution of delayed deformation with elapsed time, Fig. 6 presents the recorded axial strains normalized to the initial value recorded after immediate loading. In the observed behavior of five samples, a strain accumulation was seen to take place at a decreasing rate, eventually reaching a plateau, resembling the response of the untreated state (SLS-0-400). Conversely, 4 samples, marked on Fig. 6, were seen to yield at certain points in time where the stabilization was reversed to create an accelerating strain rate before stagnating again. In such instances, a constant load in time resulted in a delayed punctual deformation, similar to an increase in stress, but of a smaller magnitude.

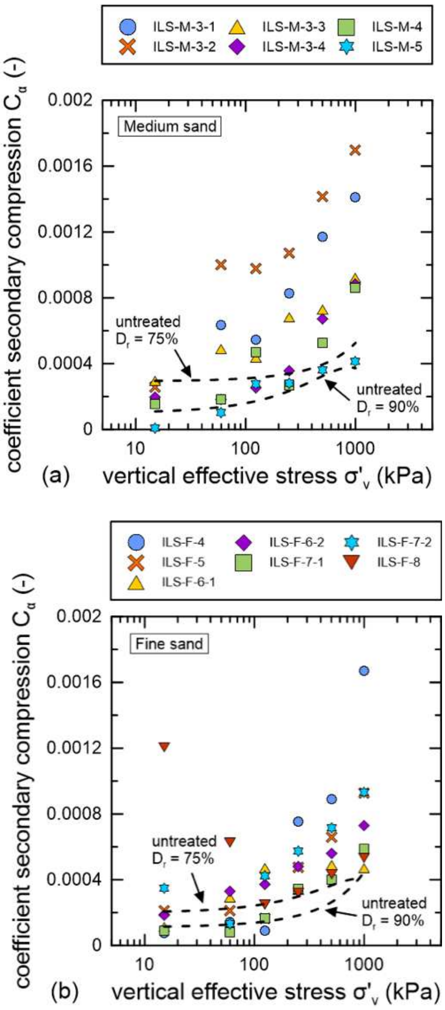

Figure 5. Variation of the coefficient of secondary compression with vertical effective stress for (a) medium and (b) fine-grained sands

4 DISCUSSIONS

In order to bring together the stress and time dependent aspects, Fig. 7, shows the variation of C_α values with the normalized preconsolidation pressure to the effective vertical stress of each loading step (p'_c/σ'_v), where C_α values are shown to rapidly increase after the applied stress exceeds p'_c of each sample. This observation between the theoretical onset of damage and an accelerating creep response, highlights the interdependence between stress and time related phenomena, as the latter cannot be dissociated from structural damage in the fabric, itself conveyed to a sample by the MICP treatment. Similar concepts are proposed in other works, where the response is differentiated in stages, prior and after the initiation of bond breakage (Xiao et al. 2020).

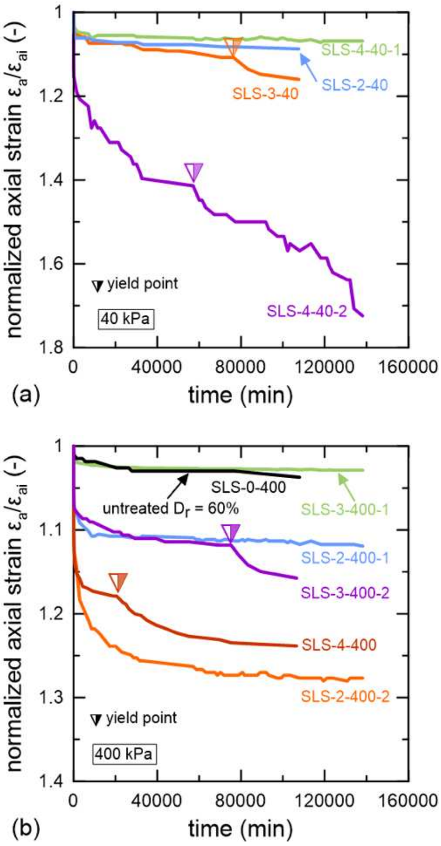

Figure 6. Normalized axial strain for a sustained effective vertical stress of (a) 40 kPa and (b) 400 kPa

More generally, stress-strain-time relations of soils are often regarded as a sum of two structural deformation mechanisms: sliding deformation or particle rearrangement, and cataclastic deformation or particle crushing. In the case of a structured sand following an MICP treatment, a peculiar quartz-calcite matrix with different properties is formed. In their pure geologic forms, their shear moduli are comparable while the bulk modulus of calcite is twice that of quartz. Still, calcite bonds produced through an MICP treatment should not be considered as geologic calcite, due to complex nucleation and growth processes, resulting in different $CaCO_3$ forms and in micro-flaws and weak planes (De Yoreo et al. 2015). As such, more cataclastic deformation is possible in the biogenic $CaCO_3$ in the matrix. This was observed in the SLS, where the delayed yield events were not strictly aligned with a treatment level nor the applied stress, but were rather governed by the presence of flaws in the calcium carbonate as is often the case even in tests dealing with mineralogical calcite (Croizé et al. 2010). From another aspect, the dominant mechanism in the origin of creep in natural sands was validated as the sliding at intergranular contacts (Andò et al. 2019). Since MICP preserves the initial configuration of a soil as a non-intrusive treatment strategy, a treated sample thus retains the same potential for grain rearrangement as its untreated state. Unlike the natural sand which dissipates this potential almost immediately after being loaded, resulting in no further deformation with time, loading a treated sand only partially rearranges its soil skeleton, leaving a potential for grain sliding, which can be later released upon further destruction of cementing bonds, as illustrated in the schematic in Fig. 8. Hence, the root of creep in MICP treated sands is not conveyed by a viscous ductility in the precipitated calcium carbonate crystals, but rather their breakage with different loading configurations: (i) increasing stresses, (ii) sustained loading, or even (iii) unloading-reloading at a stress level exceeding p'_c (observed at 500 kPa).

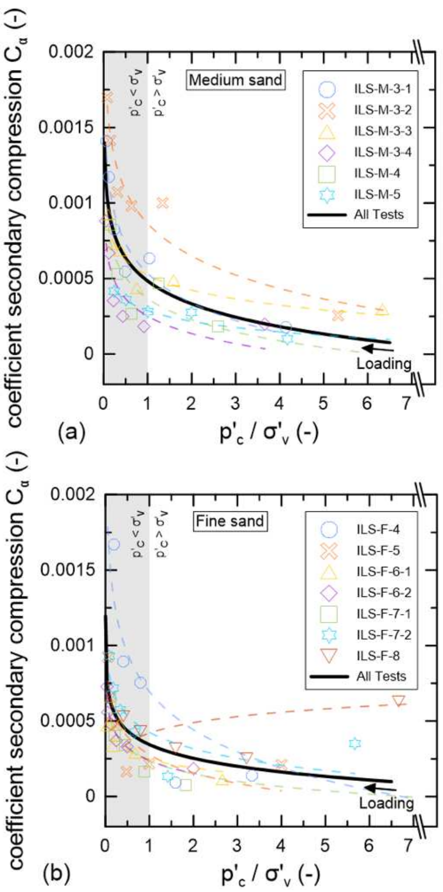

Figure 7. Variation of the coefficient of secondary compression with p'_c/σ'_v ratio for (a) medium and (b) fine-grained sands

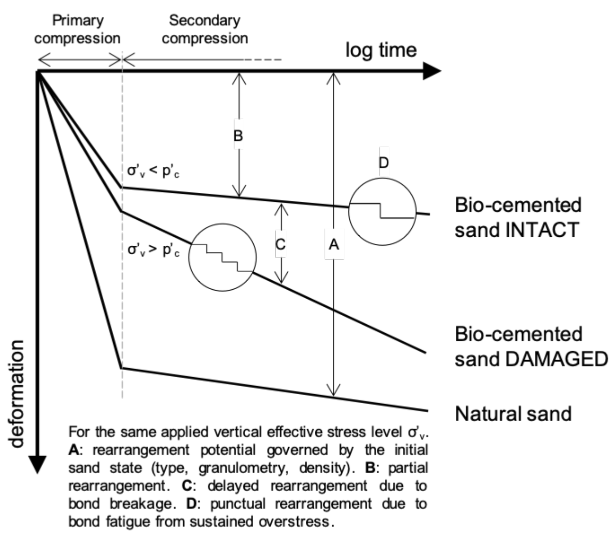

Figure 8. Schematic trends summary of natural and bio-cemented sands behaviors

5 CONCLUSIONS

Results of this work verified the enhanced compressibility of two sands with MICP treatment, in addition to investigating the permanence of the enhancement with increasing stresses and elapsed time. With increasing stress, a degradation front was seen to progressively negate the positive role of active bonds in the soil matrix, gradually debonding the structure in the sand whose response eventually depended on its initial conditions (compacity, granulometry and sand type) without immediate collapse. The existing porosity to cement ratio was compatible with the medium-grained sand. For a sustained load in time, delayed debonding events were captured to take place, while more generally under high stresses, the proportion of secondary compression to the overall deformation increased. Such time dependent observations cannot be dissociated from stress considerations, with two different regimes depending on the yield limit. The MICP treatment is herein understood as shifting a portion of the immediate settlement dictated by the natural state to be released as delayed rearrangement, not due to a viscous flow of the precipitated calcium carbonate, but rather due to its breakage with different loading configurations.

6 ACKNOWLEDGEMENTS

This work has received funding from the European Research Council (ERC) under the European Union's Horizon 2020 research and innovation program (grant agreement No. 788587).

7 REFERENCES

Andò, E., Dijkstra, J., Roubin, E., Dano, C., and Boller, E. 2019. A peek into the origin of creep in sand. *Granular Matter*, Springer Berlin Heidelberg, 21(1), 1–8.

Consoli, N. C., da Fonseca, A. V., Silva, S. R., Cruz, R. C., and Fonini, A. 2012. Parameters controlling stiffness and strength of artificially cemented soils. *Geotechnique*, 62(2), 177–183.

Croizé, D., François, R., Knut, B., and Dag Kristian, D. 2010. Experimental calcite dissolution under stress: Evolution of grain contact microstructure during pressure solution creep. *Journal of Geophysical Research*, 115.

Feng, K., and Montoya, B. M. 2014. Behavior of Bio-Mediated Soil in k0 Loading. *New Frontiers in Geotechnical Engineering GSP 243 © ASCE*, 1–10.

Lee, M. L., Ng, W. S., and Tanaka, Y. 2013. Stress-deformation and compressibility responses of bio-mediated residual soils. *Ecological Engineering*, Elsevier B.V., 60, 142–149.

Lin, H., Suleiman, M. T., Brown, D. G., and Kavazanjian, E. 2016. Mechanical behavior of sands treated by microbially induced carbonate precipitation. *Journal of Geotechnical and Geoenvironmental Engineering*, 142(2), 1–13.

Montoya, B. M., Safavizadeh, S., and Gabr, M. A. 2019. Enhancement of Coal Ash Compressibility Parameters Using Microbial-Induced Carbonate Precipitation. *Journal of Geotechnical and Geoenvironmental Engineering*, 145(5), 04019018-1–14.

Terzis, D., and Laloui, L. 2018. 3-D micro-architecture and mechanical response of soil cemented via microbial-induced calcite precipitation. *Scientific Reports*, Springer US, 8(1), 1–11.

Terzis, D., and Laloui, L. 2019. Cell-free soil bio-cementation with strength, dilatancy and fabric characterization. *Acta Geotechnica*, Springer Berlin Heidelberg, 3.

Wei, X., and Ku, T. 2020. New design chart for geotechnical ground improvement: characterizing cement-stabilized sand. *Acta Geotechnica*, Springer Berlin Heidelberg, 15(4), 999–1011.

Xiao, Y., Zhao, C., Sun, Y., Wang, S., Wu, H., Chen, H., and Liu, H. 2020. Compression behavior of MICP-treated sand with various gradations. *Acta Geotechnica*, Springer Berlin Heidelberg, 2, 1–10.

De Yoreo, J. J., Gilbert, P. U. P. A., Sommerdijk, N. A. J. M., Penn, R. L., Whitelam, S., Joester, D., Zhang, H., Rimer, J. D., Navrotsky, A., Banfield, J. F., Wallace, A. F., Michel, F. M., Meldrum, F. C., Cölfen, H., and Dove, P. M. 2015. Crystallization by particle attachment in synthetic, biogenic, and geologic environments.

Science, 349(6247), 6760.1-6760.8.

Yun, T. S., and Santamarina, J. C. 2005. Decementation, Softening, and Collapse: Changes in Small-Strain Shear Stiffness in k0 Loading. *Journal of Geotechnical and Geoenvironmental Engineering*, 131(3)(March), 350–358.